INSTITUTE OF PHYSICS PUBLISHING JOURNAL OF PHYSICS B: ATOMIC, MOLECULAR AND OPTICAL PHYSICS

J. Phys. B: At. Mol. Opt. Phys. **38** (2005) 1977–1986 doi:10.1088/0953-4075/38/12/012

Electron transfer in collisions of keV hydrogen atoms and ions with methane

B G Lindsay, W S Yu and R F Stebbings

Department of Physics and Astronomy, and Rice Quantum Institute, Rice University, 6100 Main St., Houston, TX 77005-1892, USA

Received 14 March 2005, in final form 21 April 2005
Published 6 June 2005
Online at stacks.iop.org/JPhysB/38/1977

Abstract

Absolute differential cross sections are reported for electron capture and loss by 1–5 keV H atoms incident on CH_4 for laboratory scattering angles up to 1.62°, and for charge transfer of 0.5–5 keV H^+ with CH_4 for scattering angles up to 2.09°. Electron-loss collisions are seen to result in comparatively large scattering angles and a very clear similarity exists between the present differential cross sections and those reported for other molecular targets. The present charge-transfer differential cross sections are consistent with that of Gao *et al* (1990 *Phys. Rev.* A **41** 5929–33) but not with the calculations of Kimura *et al* (1995 *Phys. Rev.* A **52** 1196–205). Prior experimental studies of electron-loss and charge-transfer are generally in good accord with the integral values reported here as are the calculations of Kusakabe *et al* (2000 *Phys. Rev.* A **62** 062715).

1. Introduction

Electron-transfer processes involving keV H and H^+ in collision with atoms and molecules have garnered considerable attention over the years because of their fundamental nature and practical importance. Collisions involving CH_4 are especially significant for plasma processing, fusion reactors and astrophysics (Janev 1995, Kusakabe *et al* 2000, Janev and Reiter 2002). To date, however, the great majority of studies have focused only on the charge transfer process (Chambers 1965, Desesquelles *et al* 1966, Koopman 1968, McNeal 1970, Berkner *et al* 1970, Eliot 1977, Rudd *et al* 1983, Jones *et al* 1985, Gao *et al* 1990, Kusakabe *et al* 2000), while data on electron loss are relatively sparse (McNeal 1970, Eliot 1977, Smith *et al* 1976, Sanders *et al* 2003), and there are no published electron capture measurements at all. Furthermore, the only prior differential cross section (DCS) measurement that we are aware of is the 1.5 keV DCS of Gao *et al* (1990). In this study we seek to redress some of these deficiencies by presenting integral cross sections and the corresponding DCSs for electron capture and loss by 1–5 keV H atoms incident on CH_4 for laboratory scattering angles between 0.020° and

1.62°, and for charge transfer of 0.5–5 keV H^+ with CH_4 for scattering angles between 0.026° and 2.09°.

One topical area of potential application for these measurements is analysis of the data returned by the Cassini–Huygens space mission (Matson *et al* 2002). The present data are, however, only likely to be relevant to the very lowest energy energetic neutral atom observations (Krimigis *et al* 2004).

2. Apparatus and experimental procedure

Both the H-atom electron-capture and -loss measurements and the H^+ charge transfer measurements were performed using the same apparatus. Although the techniques used were quite similar, there are significant differences and the experimental procedures are described separately.

The experimental method used to obtain the H-atom cross sections has been described in detail previously (Smith *et al* 1991, Lindsay *et al* 2004). H_2 is admitted to a magnetically confined plasma ion source. Ions are extracted from the source, accelerated and focused to form a beam of the desired energy. A pair of 60°-sector magnets is used to select H^+ ions which then enter a charge-transfer cell (CTC) where some of them are converted to fast neutral H atoms via charge transfer with krypton. At the energies studied here, the near-resonant H^+–Kr charge transfer reaction produces predominantly ground-state atoms. A strong transverse electric field removes residual ions and also serves to quench any metastables that may be present (Smith *et al* 1991). The neutral H-atom beam is collimated to an angular divergence of 0.006° by passage through a pair of laser-drilled apertures that form the exit of the CTC and the entrance to the target cell (TC). Following passage through the short target cell, the H-atom beam impacts a position-sensitive detector (PSD1), which is located 68 cm beyond it. A second set of deflection plates is utilized to deflect fast product ions emerging from the target cell through an angle of approximately 5° onto a second position-sensitive detector (PSD2).

To measure the differential electron-capture or -loss cross section, CH_4 is admitted to the target cell and the angles of scatter of the H^- or H^+ ions, formed through electron capture or loss by the primary H atoms, are determined from their positions of impact on PSD2. The H-atom flux incident on the target is determined by combining the number of H atoms that impact PSD1 with the number of ions produced. These measurements, together with the target number density, the target length and the relative detection efficiency of the two PSDs, are sufficient to determine the absolute differential and integral cross sections.

The target number density n is obtained from pressure measurements using an MKS Baratron absolute capacitance diaphragm gauge. Earlier studies demonstrated that the effective length of the gas target was accurately given by l the physical length of the target cell (Newman *et al* 1985), and that the target thickness is given by the product of n and l. Evaluation of the PSDs' relative detection efficiency requires careful consideration of the detectors' characteristics (Gao *et al* 1984, Straub *et al* 1999) and is accomplished by alternately deflecting an H^+ ion beam onto PSD1 and PSD2 (Lindsay *et al* 2004). In practice, PSD2's detection efficiency is found to be within about 10% of that for PSD1 at all of the energies studied.

Since the measured cross sections are generally small compared to those for reneutralization of the charged products, it is necessary to maintain conditions in the target cell so that the probability that a charged product ion is reneutralized is low. To this end, the pressure in the 1.51-mm-long target cell is maintained at less than 15 mTorr, which allows for reasonable count rates while limiting secondary collisions to a tolerable level. Corrections of

up to 10% are made to the electron-loss cross sections, utilizing the present charge transfer cross section data, to account for the loss of H^+ ions via charge transfer. It is, however, not feasible to similarly correct the H-atom electron-capture cross sections because of the lack of appropriate electron-loss data for H^- ions. The available data, which are for electron loss by H^- ions with other gaseous targets (Nakai *et al* 1987), suggest that the magnitude of the electron-capture cross section correction is similar to that for the electron-loss measurements.

Due to the finite angular range subtended by the detector, collection of all fast ionic products is not possible. The extent to which the integral cross section approximates the total cross section may, however, be gauged from the rapidity with which the DCS decreases as the scattering angle increases. Such an analysis indicates that the present integral electron capture cross sections are a very good approximation to the total cross sections and, in the worst case, approach the total cross sections to within better than 10%. The situation for the electron-loss data is not as clear cut: a similar analysis indicates that, at energies of 2 keV and greater, the present integral cross sections are not more than 25% smaller than the total cross sections. The 1 keV integral electron-loss cross section should, however, only be regarded as a lower limit to the total cross section.

The experimental method employed for the H^+ charge transfer measurements is the same as that described in detail previously by Lindsay *et al* (1996), except that the flow system arrangement they employed is not used here. A proton beam is generated as described above, however, for charge transfer, the CTC is evacuated and no transverse electric field is used. The collimated proton beam therefore passes through the target cell and impacts PSD1. PSD1 serves to measure the flux of protons passing through the target cell and also to measure the scattered H-atom products. Note that, since PSD1 is physically smaller than PSD2, it is repositioned closer to the target cell so that data are collected over a comparable angular range to the electron-capture and -loss measurements.

In order to measure the differential charge-transfer cross section CH_4 is admitted to the target cell and the angles of scatter of the neutral H atoms, formed by charge transfer of the primary H^+ ions, are determined from their positions of impact on PSD1. Unscattered primary H^+ ions are normally deflected away from PSD1, using deflection plates positioned just beyond the target cell, but are allowed to impact it periodically to assess the primary beam flux. These measurements, together with the target number density, obtained from the target gas pressure, and target length are sufficient to determine the absolute DCS. Note that the detection efficiencies of H^+ and H are identical to within experimental uncertainties (Gao *et al* 1988, Johnson *et al* 1989)

3. Results and discussion

The measured differential electron-capture and -loss cross sections are shown in figure 1 and selected values are tabulated in table 1. Besides the statistical uncertainties shown on the graphs there are additional systematic uncertainties that range from $\pm 10\%$ to $\pm 27\%$ (table 2). The angular uncertainties arise from the finite primary beam size and the angular resolution used for analysis. From figure 1 it can be seen that all of the DCSs are forward peaked and that electron-capture collisions generally result in smaller scattering angles than electron-loss collisions. The slow decrease of the cross section with angle seen in the 1 keV electron-loss DCS indicates that a not inconsequential fraction of the colliding particles are deflected through quite large angles. The lack of structure in the DCSs—which all decrease monotonically with angle—may perhaps be attributable to the complexity of the collision system which, of course, involves six atoms.

Table 1. Laboratory frame differential H–CH_4 electron-loss and electron-capture cross sections, where E is the projectile energy and the numbers in square brackets represent powers of 10.

	$d\sigma(\theta)/d\Omega$ (10^{-16} cm^2 sr^{-1})							
Laboratory	Electron-loss, σ_{01}				Electron-capture, σ_{0-1}			
angle θ (°)	$E = 1$ keV	$E = 2$ keV	$E = 3$ keV	$E = 5$ keV	$E = 1$ keV	$E = 2$ keV	$E = 3$ keV	$E = 5$ keV
0.020 ± 0.015	9.14 ± 1.82[3]	3.08 ± 0.34[4]	7.57 ± 0.55[4]	1.78 ± 0.08[5]	5.08 ± 1.39[3]	4.58 ± 0.41[4]	1.08 ± 0.09[5]	1.43 ± 0.10[5]
0.048 ± 0.015	7.20 ± 1.08[3]	2.75 ± 0.22[4]	5.76 ± 0.31[4]	9.63 ± 0.39[4]	4.33 ± 0.83[3]	3.37 ± 0.22[4]	7.10 ± 0.48[4]	8.14 ± 0.49[4]
0.075 ± 0.015	6.23 ± 0.81[3]	2.00 ± 0.15[4]	3.83 ± 0.20[4]	5.21 ± 0.23[4]	3.40 ± 0.58[3]	1.79 ± 0.13[4]	2.83 ± 0.24[4]	2.15 ± 0.20[4]
0.116 ± 0.015	3.83 ± 0.55[3]	1.32 ± 0.10[4]	1.66 ± 0.11[4]	2.06 ± 0.12[4]	2.45 ± 0.42[3]	6.39 ± 0.63[3]	9.56 ± 1.14[3]	5.94 ± 0.90[3]
0.157 ± 0.015	4.24 ± 0.47[3]	8.24 ± 0.66[3]	9.72 ± 0.71[3]	1.15 ± 0.08[4]	1.47 ± 0.27[3]	3.27 ± 0.42[3]	3.38 ± 0.61[3]	1.85 ± 0.45[3]
0.198 ± 0.015	3.32 ± 0.38[3]	5.24 ± 0.48[3]	6.97 ± 0.56[3]	6.56 ± 0.52[3]	6.64 ± 1.80[2]	1.30 ± 0.26[3]	1.59 ± 0.40[3]	9.78 ± 3.19[2]
0.252 ± 0.015	1.99 ± 0.28[3]	3.75 ± 0.36[3]	4.87 ± 0.42[3]	3.61 ± 0.35[3]	3.36 ± 1.52[2]	9.49 ± 2.08[2]	8.19 ± 2.80[2]	2.90 ± 2.34[2]
0.320 ± 0.025	1.42 ± 0.13[3]	2.13 ± 0.15[3]	2.28 ± 0.15[3]	2.45 ± 0.15[3]	1.38 ± 0.69[2]	3.43 ± 0.78[2]	2.44 ± 1.09[2]	7.33 ± 7.33[1]
0.402 ± 0.025	9.64 ± 1.02[2]	1.34 ± 0.11[3]	1.37 ± 0.11[3]	1.36 ± 0.11[3]	8.08 ± 6.50[1]	2.48 ± 0.63[2]	6.74 ± 6.74[1]	–
0.484 ± 0.025	8.22 ± 0.84[2]	9.35 ± 0.92[2]	1.05 ± 0.09[3]	7.49 ± 0.84[2]	1.08 ± 0.52[2]	6.98 ± 5.49[1]	–	9.52 ± 4.63[1]
0.607 ± 0.025	3.89 ± 0.70[2]	6.84 ± 0.77[2]	5.61 ± 0.73[2]	4.01 ± 0.62[2]	9.62 ± 4.77[1]	7.39 ± 4.87[1]	–	4.74 ± 4.72[1]
0.893 ± 0.025	2.21 ± 0.52[2]	1.73 ± 0.50[2]	2.99 ± 0.54[2]	2.62 ± 0.52[2]	–	–	–	–
1.405 ± 0.056	1.07 ± 0.23[2]	6.40 ± 2.33[1]	–	–	–	–	–	–

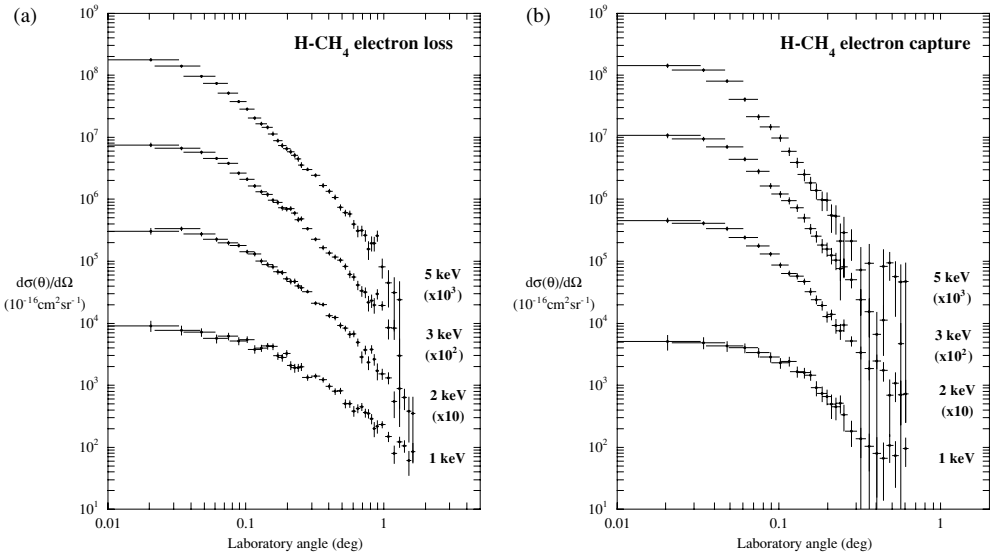

Figure 1. (a) Absolute differential cross sections for electron-loss by H atoms in collisions with CH_4. (b) Absolute differential cross sections for electron-capture by H atoms in collisions with CH_4. For convenience of presentation the data have been multiplied by the factors indicated.

Table 2. Absolute integral electron-transfer cross sections for H atoms and H^+ ions with CH_4. The angular range for the integral H-atom cross sections is 0–1.79°, and that for the charge transfer cross sections is 0–2.51°. Note that these angular ranges are somewhat greater than those over which DCSs are reported because the statistical quality of the DCS data at the largest angles is generally poor.

Energy (keV)	H-atom electron loss, σ_{01} (10^{-16} cm^2)	H-atom electron capture, $\sigma_{0\text{-}1}$ (10^{-17} cm^2)	H^+ charge-transfer, σ_{10} (10^{-16} cm^2)
0.5			24.7 ± 2.7
1	0.83 ± 0.10	1.25 ± 0.34	23.8 ± 2.1
2	1.24 ± 0.14	4.58 ± 0.85	22.3 ± 1.3
3	1.51 ± 0.16	6.31 ± 0.93	21.5 ± 1.3
5	1.70 ± 0.17	5.70 ± 0.84	18.6 ± 1.1

There do not appear to be any other electron-capture or -loss data with which the present results may be directly compared, but, when the present electron-loss DCSs are compared to those for other molecular targets, a significant degree of similarity is observed. This is illustrated in figure 2, where the present data are compared to the H–N_2 measurements of Smith *et al* (1991). The most striking feature seen in the figure is the manner in which all of the DCSs coalesce into a single curve at larger angles. The angular dependence of the cross sections is also seen to approach that for H–N_2 direct scattering (Newman *et al* 1986, Johnson *et al* 1988). This behaviour may be explained by considering that large angle scattering implies rather violent small-impact-parameter collisions between the hydrogen nucleus and the target, and that it is primarily this strong interaction that determines the DCS (Van Zyl *et al* 1977).

The present integral cross sections and their associated uncertainties are tabulated in table 2. The uncertainties principally arise from the relative efficiency calibration of the

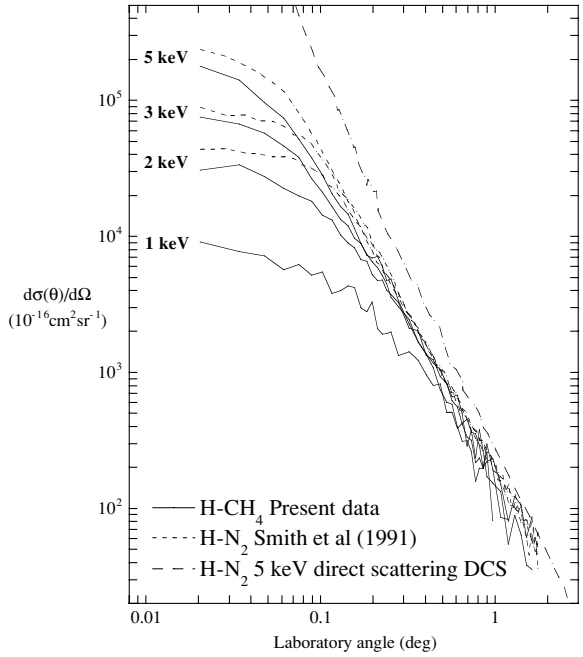

Figure 2. Comparison of the present H–CH_4 electron-loss DCSs with those for H–N_2 reported by Smith *et al* (1991). The H–N_2 direct scattering cross section is also shown (Newman *et al* 1986, Johnson *et al* 1988).

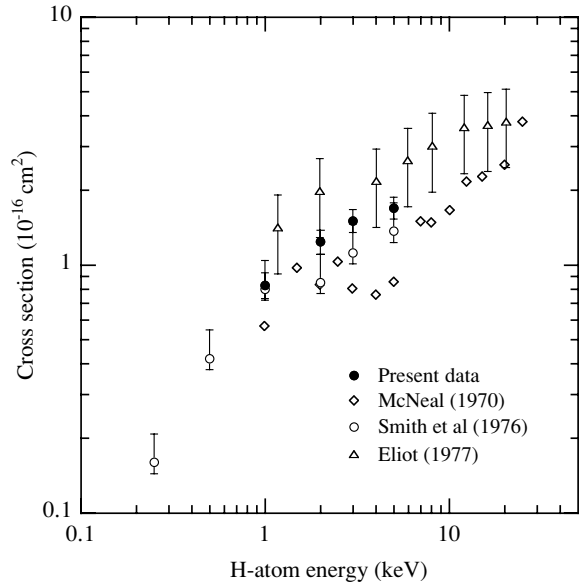

Figure 3. Integral cross sections for electron-loss by H atoms in collisions with CH_4. Previous total cross section measurements are shown for comparison.

two PSDs, the uncertainty in the ratio of the H^+ to H-atom detection efficiencies, and to the repeatability of the measurements. Figure 3 shows how the electron-loss cross sections

Table 3. Laboratory frame differential H^+–CH_4 charge-transfer cross sections, where E is the projectile energy and the numbers in square brackets represent powers of 10.

Laboratory angle, θ (°)	$d\sigma(\theta)/d\Omega$ (10^{-16} cm^2 sr^{-1})				
	$E = 0.5$ keV	$E = 1$ keV	$E = 2$ keV	$E = 3$ keV	$E = 5$ keV
0.026 ± 0.016	6.99 ± 0.19[5]	1.35 ± 0.03[6]	3.18 ± 0.04[6]	4.54 ± 0.05[6]	5.54 ± 0.05[6]
0.044 ± 0.016	7.85 ± 0.16[5]	1.55 ± 0.02[6]	2.89 ± 0.03[6]	3.37 ± 0.03[6]	3.25 ± 0.03[6]
0.061 ± 0.016	7.72 ± 0.14[5]	1.22 ± 0.02[6]	1.52 ± 0.02[6]	1.29 ± 0.02[6]	9.57 ± 0.13[5]
0.096 ± 0.016	4.32 ± 0.08[5]	2.73 ± 0.06[5]	3.36 ± 0.07[5]	3.97 ± 0.08[5]	2.77 ± 0.05[5]
0.131 ± 0.016	1.39 ± 0.04[5]	3.27 ± 0.06[5]	3.46 ± 0.06[5]	1.79 ± 0.04[5]	8.61 ± 0.26[4]
0.167 ± 0.016	1.45 ± 0.04[5]	2.53 ± 0.04[5]	8.77 ± 0.28[4]	6.51 ± 0.23[4]	4.59 ± 0.17[4]
0.202 ± 0.016	1.30 ± 0.03[5]	7.87 ± 0.22[4]	6.43 ± 0.22[4]	4.15 ± 0.17[4]	2.18 ± 0.11[4]
0.237 ± 0.016	6.03 ± 0.19[4]	8.84 ± 0.22[4]	3.86 ± 0.16[4]	2.12 ± 0.11[4]	1.38 ± 0.08[4]
0.272 ± 0.016	4.78 ± 0.16[4]	7.55 ± 0.19[4]	1.91 ± 0.10[4]	1.24 ± 0.08[4]	9.43 ± 0.62[3]
0.307 ± 0.016	5.57 ± 0.16[4]	3.76 ± 0.13[4]	1.34 ± 0.08[4]	8.54 ± 0.64[3]	7.06 ± 0.50[3]
0.359 ± 0.029	3.66 ± 0.07[4]	2.45 ± 0.05[4]	8.37 ± 0.34[3]	5.83 ± 0.28[3]	4.22 ± 0.21[3]
0.465 ± 0.029	2.42 ± 0.05[4]	8.89 ± 0.29[3]	3.58 ± 0.20[3]	2.89 ± 0.17[3]	2.26 ± 0.14[3]
0.622 ± 0.029	1.09 ± 0.03[4]	2.66 ± 0.14[3]	1.30 ± 0.11[3]	1.17 ± 0.10[3]	1.05 ± 0.08[3]
0.780 ± 0.029	4.84 ± 0.18[3]	1.31 ± 0.09[3]	7.55 ± 0.78[2]	8.08 ± 0.78[2]	5.95 ± 0.56[2]
0.991 ± 0.029	1.80 ± 0.10[3]	7.59 ± 0.62[2]	3.85 ± 0.52[2]	4.37 ± 0.51[2]	2.20 ± 0.38[2]
1.245 ± 0.071	8.36 ± 0.38[2]	3.16 ± 0.25[2]	2.53 ± 0.24[2]	2.10 ± 0.21[2]	1.63 ± 0.17[2]
1.666 ± 0.071	1.87 ± 0.20[2]	1.66 ± 0.19[2]	1.32 ± 0.21[2]	9.79 ± 1.85[1]	5.91 ± 1.29[1]
2.086 ± 0.071	1.32 ± 0.21[2]	8.34 ± 1.87[1]	6.27 ± 1.92[1]	6.44 ± 1.88[1]	3.12 ± 1.32[1]
2.507 ± 0.071	7.49 ± 1.68[1]	4.58 ± 2.05[1]	–	4.12 ± 1.91[1]	–

compare to the previous total measurements of McNeal (1970), Smith *et al* (1976) and Eliot (1977). Note that the uncertainty associated with the McNeal (1970) data is ±50% or more, and that the high-energy measurements of Toburen *et al* (1968) and Sanders *et al* (2003) are not shown. The overall agreement between the various measurements is seen to be quite good, especially given the uncertainties involved. The energy dependence of the cross section is consistent with what has been observed for other collision systems (Lindsay *et al* 2004) and with the highly endothermic nature of the reaction. Although it is not possible to directly compare the data in the figure with the high-energy data of Toburen *et al* (1968) and Sanders *et al* (2003), it is worth pointing out that these two studies are in excellent agreement with each other and appear to be consistent with the low-energy data. To our knowledge, there are no electron-capture data with which the present measurements may be compared.

The measured differential charge-transfer cross sections are shown in figure 4 and selected values are tabulated in table 3. Besides the statistical uncertainties shown on the graphs there are additional systematic uncertainties that range from ±6% to ±11% (table 2). All of the DCSs are strongly forward peaked as might be expected for a collision system where small energy defects are involved. The structure seen in the DCSs corresponding to the three lowest energies studied has been attributed to a combination of interference effects by Gao *et al* (1990); their 1.5 keV DCS data are shown for comparison with the present 2 keV curve. The 3- and 5 keV curves lack any structure, in all likelihood because of the many competing reaction channels that are available at these energies.

The 1.5 keV DCS calculated by Kimura *et al* (1995) using a molecular orbital expansion technique within a fully quantum-mechanical formalism is also shown in figure 4. Clearly, above 0.1° the agreement is not particularly good; the sharp fall in the calculated DCS at

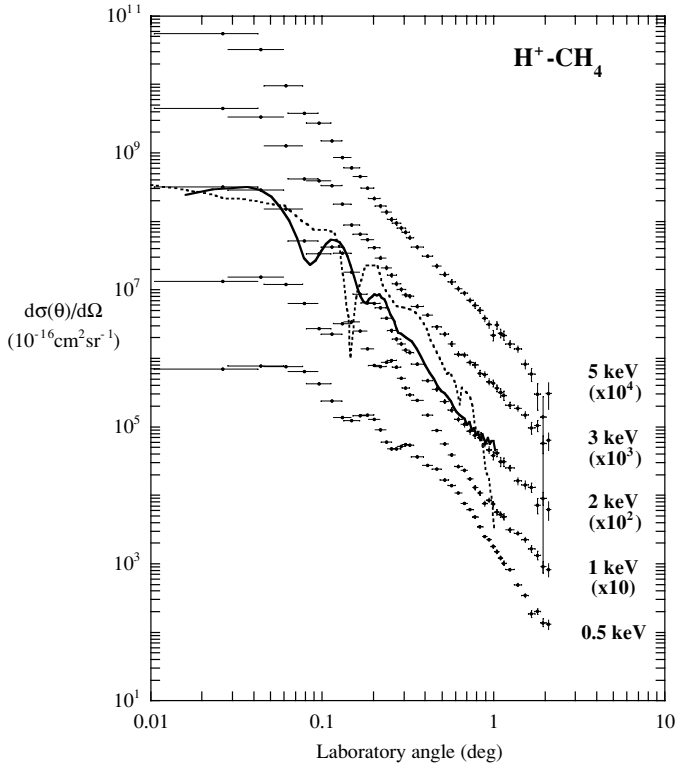

Figure 4. Absolute differential cross sections for charge transfer of H^+ with CH_4. The 1.5 keV measurement of Gao *et al* (1990) (solid line) and the calculations of Kimura *et al* (1995) (dashed line) are plotted for comparison. For convenience of presentation the data have been multiplied by the factors indicated.

about 1° is not reproduced by the data of Gao *et al* (1990) and the present study confirms that the angular dependence reported by Gao *et al* (1990) is maintained to angles much greater than 1°.

The strongly forward peaked nature of the charge-transfer DCSs indicates that essentially all of the scattered H-atom products are detected, the fraction missed constituting a few per cent at most. The integral cross sections are therefore, for all practical purposes, equal to total cross sections and may be directly compared to prior measurements (figure 5). Not shown in the figure are high-energy measurements (Desesquelles *et al* 1966, Toburen *et al* 1968, Jones *et al* 1985, Sanders *et al* 2003) and those subject to very large uncertainties (Collins and Kebarle 1967). The excellent agreement between the present measurements and those of Berkner *et al* (1970) and the more recent data of Kusakabe *et al* (2000) is particularly noteworthy. The high-energy measurements (Desesquelles *et al* 1966, Toburen *et al* 1968, Jones *et al* 1985, Sanders *et al* 2003) and the integral cross section reported by Gao *et al* (1990) (2.3×10^{-15} cm^2) are consistent with the measurements shown.

Also shown in figure 5 are the H^+–CH_4 calculations of Kusakabe *et al* (2000) obtained using the molecular orbital (MO) expansion method and those obtained by applying the Olson formula (Olsen *et al* 1971, Olsen 1972, Olsen and Smith 1973, Ice and Olsen 1975). If one considers that the cross section is best represented by the present measurements together with

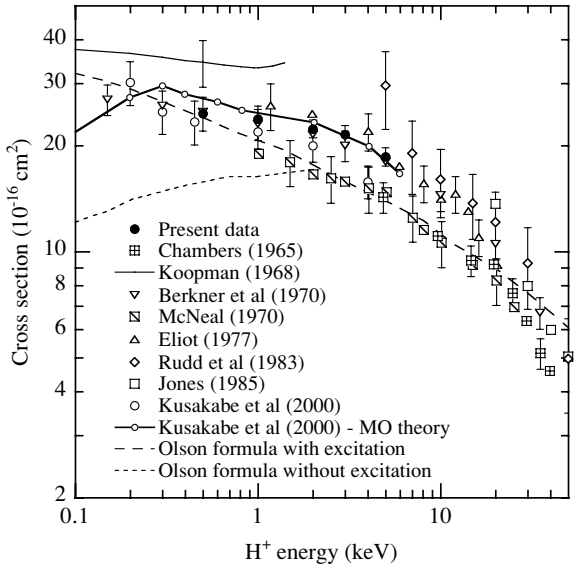

Figure 5. Integral cross sections for charge transfer of H^+ with CH_4 together with previous total cross section measurements. Berkner *et al* (1970) actually measured cross sections for D^+ and their data are plotted at the equivalent proton energy. The Olson formula calculations are from Kusakabe *et al* (2000) and are shown with and without vibrational excitation of the product molecular ion.

those of Kusakabe *et al* (2000) and of Berkner *et al* (1970), as seems reasonable, then the MO calculations are much superior to what has gone before.

4. Conclusion

Absolute differential and integral cross sections are reported for electron capture and loss by 1–5 keV H atoms incident on CH_4, and for charge transfer of 0.5–5 keV H^+ with CH_4. A significant fraction of the fast electron-loss products are observed to scatter through relatively large angles at the lowest energies and a conspicuous similarity is noted between the present electron-loss DCSs and those reported for other targets. The large-angle behaviour of the electron-loss DCSs is consistent with violent small-impact-parameter collisions between the hydrogen nucleus and the target. The published electron-loss total cross sections agree quite well with the present measurements, particularly given the uncertainties involved.

The strongly forward peaked charge-transfer DCSs are consistent with the only comparable study (Gao *et al* 1990), but notable disagreements exist between the experimental data and the calculations of Kimura *et al* (1995). Prior total cross section measurements are generally in very good agreement with the present data and the MO calculations of Kusakabe *et al* (2000) are in excellent agreement with them.

Acknowledgments

We gratefully acknowledge support by the Robert A Welch Foundation (under Grant no. C-0552) and by the National Science Foundation (under Grant no. 0108734), which funded development of the apparatus. We would also like to acknowledge useful communications with Pontus Brandt.

References

Berkner K H, Pyle R V and Stearns J W 1970 *Nucl. Fusion* **10** 145–9
Chambers E S 1965 *Report No. UCRL-14214* University of California 1–16
Collins J G and Kebarle P 1967 *J. Chem. Phys.* **46** 1082–9
Desesquelles J, Cao G D and Dufay M 1966 *Compt. Rend.* **262B** 1329–32
Eliot M 1977 *J. de Physique* **38** 21–7
Gao R S, Gibner P S, Newman J H, Smith K A and Stebbings R F 1984 *Rev. Sci. Instrum.* **55** 1756–9
Gao R S, Johnson L K, Schafer D A, Newman J H, Smith K A and Stebbings R F 1988 *Phys. Rev.* A **38** 2789–93
Gao R S, Johnson L K, Hakes C L, Smith K A and Stebbings R F 1990 *Phys. Rev.* A **41** 5929–33
Ice G E and Olson R E 1975 *Phys. Rev.* A **11** 111–8
Janev R K (ed) 1995 *Atomic and Molecular Processes in Fusion Edge Plasmas* (New York: Plenum) pp 1–13
Janev R and Reiter D 2002 *Phys. Plasmas* **9** 4071–81
Johnson L K, Gao R S, Smith K A and Stebbings R F 1988 *Phys. Rev.* A **38** 2794–7
Johnson L K, Gao R S, Hakes C L, Smith K A and Stebbings R F 1989 *Phys. Rev.* A **40** 4920–5
Jones M L, Doughty B M, Dillingham T R and Jones T A 1985 *Nucl. Instrum. Methods* B **10** 142–5
Kimura M, Li Y, Hirsch G and Buenker R J 1995 *Phys. Rev.* A **52** 1196–205
Koopman D W 1968 *J. Chem. Phys.* **49** 5203–5
Krimigis S M *et al* 2004 *Space Sci. Rev.* **114** 233–329
Kusakabe T, Asahina K, Iida A, Tanaka Y, Li Y, Hirsch G, Buenker R J, Kimura M, Tawara H and Nakai Y 2000 *Phys. Rev.* A **62** 062715
Lindsay B G, Sieglaff D R, Schafer D A, Hakes C L, Smith K A and Stebbings R F 1996 *Phys. Rev.* A **53** 212–8
Lindsay B G, Yu W S, McDonald K F and Stebbings R F 2004 *Phys. Rev.* A **70** 042701
Matson D L, Spilker L J and Lebreton J-P 2002 *Space Sci. Rev.* **104** 1–58
McNeal R J 1970 *J. Chem. Phys.* **53** 4308–13
Nakai Y, Shirai T, Tabata T and Ito R 1987 *At. Data Nucl. Data Tables* **37** 69–101
Newman J H, Smith K A, Stebbings R F and Chen Y S 1985 *J. Geophys. Res.* **90** 11045–54
Newman J H, Chen Y S, Smith K A and Stebbings R F 1986 *J. Geophys. Res.* **91** 8947–54
Olson R E 1972 *Phys. Rev.* A **6** 1822–30
Olson R E and Smith F T 1973 *Phys. Rev.* A **7** 1529–35
Olson R E, Smith F T and Bauer E 1971 *Appl. Opt.* **10** 1848–55
Rudd M E, DuBois R D, Toburen L H, Ratcliffe C A and Goffe T V 1983 *Phys. Rev.* A **28** 3244–57
Sanders J M, Varghese S L, Fleming C H and Soosai G A 2003 *J. Phys. B: At. Mol. Opt. Phys.* **36** 3835–46
Sieglaff D R, Lindsay B G, Smith K A and Stebbings R F 1999 *Phys. Rev.* A **59** 3538–43
Sieglaff D R, Lindsay B G, Merrill R L, Smith K A and Stebbings R F 2000 *J. Geophys. Res.* **105** 10631–5
Smith K A, Duncan M D, Geis M W and Rundel R D 1976 *J. Geophys. Res.* **81** 2231–6
Smith G J, Johnson L K, Gao R S, Smith K A and Stebbings R F 1991 *Phys. Rev.* A **44** 5647–52
Stebbings R F, Turner B R and Rutherford J A 1966 *J. Geophys. Res.* **71** 771–84
Straub H C, Mangan M A, Lindsay B G, Smith K A and Stebbings R F 1999 *Rev. Sci. Instrum.* **70** 4238–40
Toburen L H, Nakai M Y and Langley R A 1968 *Phys. Rev.* **171** 114–22
Turner B R and Rutherford J A 1968 *J. Geophys. Res.* **73** 6751–8
Van Zyl B, Le T Q, Neumann H and Amme R C 1977 *Phys. Rev.* A **15** 1871–86